# Braiding, branching and chiral amplification of nanofibres in supramolecular gels

*Christopher D. Jones[a], Henry T. D. Simmons[a], Kate E. Horner[b], Kaiqiang Liu[c], Richard L. Thompson[a] and Jonathan W. Steed[a]**

a) Department of Chemistry, Durham University, South Road, Durham, DH1 3LE. jon.steed@durham.ac.uk

b) SPOCK Group, Department of Mathematical Sciences, Durham University, South Road, Durham, DH1 3LE, UK.

c) Key Laboratory of Applied Surface and Colloid Chemistry (Ministry of Education), School of Chemistry and Chemical Engineering, Shaanxi Normal University, Xi'an China 710119.

## Abstract

Helical nanofibres play key roles in many biological processes. Entanglements between helices can aid gelation by producing thick, interconnected fibres — for example the strain-stiffening of fibrin, actin and collagen under tension — but the details of this process are poorly understood. Herein we describe the assembly of an achiral oligo(urea) peptidomimetic compound into supramolecular helices. Aggregation of adjacent helices leads to the formation of fibrils, which further intertwine to produce high-fidelity braids with periodic crossing patterns. A braid-theory analysis suggests that braiding is governed by rigid topological constraints, and that branching occurs due to crossing defects in the developing braids. Mixed-chirality helices assemble into relatively complex, odd-stranded braids, but can also form helical bundles by undergoing inversions of chirality. The oligo(urea) assemblies are also highly sensitive to chiral amplification, proposed to occur through a majority rules mechanism — trace chiral materials can promote the formation of gels containing only homochiral helices.

Many small-molecule gels consist of fibrous nanostructures comprising anisotropic supramolecular motifs, such as hydrogen bonded tapes of ureas and amides[1] or tubular micelles of amphiphilic species[2]. These interactions can be targeted by rational design of the gelator structure. However, it is often interactions between fibres that dictate the appearance and mechanical properties of a fibrous gel[3-5]. For example, helical bundles of some amyloid fibrils favour left-handed morphologies[6] but this chirality may be inverted if separate left-handed bundles are intertwined[7]. Entanglement of fibres can alter the optical characteristics of a material[8,9] and is responsible for many useful mechanical phenomena, such as the strain-stiffening of fibrin, actin and collagen under tension[10-13]. Moreover, defects in the crossing patterns of entangled fibrils give rise to nodes or branch points[14], increasing the connectivity of the fibre network and stiffness of the resulting gel[15].

Twisted fibrils tend to be morphologically uniform[16] and are thus well-suited to the formation of clearly defined entanglements[17]. Helical bundles are particularly favoured because they are topologically trivial, allowing strands to be added or removed without threading the free ends[18]. More permanent connections, analogous to the mechanical bonds of catenanes, rotaxanes and molecular knots[19,20], arise when fibrils self-assemble into braided networks[21-25]. Braids, also known as plaits and sinnets, are an important component of ropes, decorative structures and other man-made objects[26], but rarely occur in natural materials. Indeed, while biopolymers such as DNA and proteins can exhibit various knotted geometries, these are always produced by threading and linking the ends of helical bundles[27-29]. To the best of our knowledge, braiding has not been observed in materials other than molecular crystals, despite extensive research into self-assembled colloidal nanostructures[30-32].

Gels based on Low Molecular Weight Gelators (LMWGs) with biomimetic functionalities are a promising source of braided assemblies. Urea-containing LMWGs are of particular interest as they can be readily prepared from a variety of starting materials, and frequently self-assemble into continuous hydrogen-bonding arrays known as α-tape motifs. In an α-tape, each urea NH group donates to the carbonyl oxygen atom of the next molecule to form a linear chain of hydrogen bonds[33,34]. The resulting assemblies resemble peptide-based architectures, such as helical foldamers[35,36] and lamellar β-sheet assemblies[37-39], but are often more robust, predictable, and tolerant to changes in gelator structure. Mono(urea) and bis(urea) gelators have been investigated for use in catalysis[40], chemical sensing[41]

and crystal growth[42,43]. However, there have been relatively few studies focussing on the self-assembly of oligo(urea)s[44-47].

In this study, braids with nanoscale dimensions were prepared *via* the self-assembly of an achiral oligo(urea). The aim of the investigation was to determine how helix chirality influences the topology of a braid, defined as the crossing pattern of strands, and the connectivity of the gel fibre network. Braid theory[48] was used to explain the feasibility of braiding, identify the most favoured braid topologies and rationalise differences between homochiral and heterochiral helix interactions. Furthermore, gels comprising only right-handed helices were produced *via* a chiral amplification method, allowing the microstructural effects of fibril handedness to be directly visualised.

## Results and discussion

### *Self-assembly behaviour*

Compounds with one or two urea groups may self-assemble into twisted fibrils[49,50], but these are usually wider and less uniform than peptide-based structures. We hypothesised that oligo(urea)s would access conformations comparable to those of oligopeptides and generate structures with more biomimetic morphologies [51,52]. To investigate the effect of oligo(urea) length on the self-assembly outcome, carbonyl diimidazole (CDI) coupling reactions[53] were used to synthesise a tris(urea) **1** and pentakis(urea) **2** containing the same repeat unit. We observed that competitive pyridyl-urea interactions can disrupt the α-tape motifs of bis(urea) compounds[54-56], so incorporated pyridyl end groups to promote fibrous aggregates over three-dimensional hydrogen bonding networks. The compounds were found to be insoluble in most organic solvents, including the polar liquids benzyl alcohol, cyclohexanone, pyridine and acetic acid. However, both **1** and **2** dissolve in hot DMF, with ambient solubility limits of 1.0 and 0.2% (w/v), respectively. Aggregates were obtained by cooling the supersaturated solutions to room temperature and analysed by scanning electron microscopy (SEM) after drying in air.

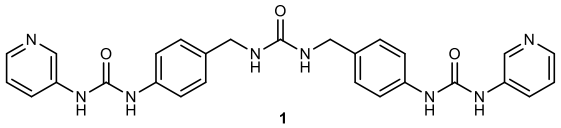

1

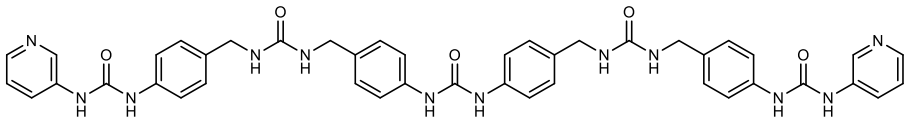

2

Compound **1** precipitates from DMF on standing, forming flat sheets of variable width and a typical thickness of 200-250 nm (Fig. 1a). Similar ribbons, 100-150 nm in width, are also observed in aggregates of compound **2**, suggesting that the molecules follow a common self-assembly mechanism. However, cooling a hot supersaturated DMF solution of **2** results in a weak gel comprising unbranched, highly entangled helical fibrils (Fig. 1b). Larger ribbon-shaped aggregates occur alongside the fibrils at all tested concentrations but represent only a small fraction of the materials, spanning less than 10% of the area of SEM micrographs (Supplementary Information Section 4). It is concluded that compound **2** favours an alternative self-assembly pathway that is inaccessible to the shorter, less flexible tris(urea) analogue.

SEM images reveal that fibrils of **2** are relatively narrow, with diameters approximately four times the length of the extended molecule. However, fibrils of like chirality frequently intertwine to form helical bundles with an estimated maximum size of 10-13 fibrils, corresponding to an overall fibre thickness of 25-30 nm. In addition, there are many examples of flat braided structures, which may exhibit complex arrangements of more than a dozen helices (Fig. 1c). The braids involve co-aligned fibrils, with equal numbers of strands entering and leaving each assembly. Most braids are relatively short, splitting and recombining at pseudo-permanent branch points to produce the sample-spanning network necessary for gelation.

Gels of **2** form over a range of concentrations. A 0.5% (w/v) gel forms over several hours, but gelation time increases to one week at the critical gelator concentration (CGC) of 0.2% (w/v). Precise rheological testing is made difficult by partial breakdown of the gels when they are transferred by spatula onto the rheometer stage. Nonetheless, the gels consistently display a typical viscoelastic response to oscillatory shear[57], with $G'$ exceeding $G''$ by an order of magnitude (Fig. 1d) and remaining approximately constant over a range of frequencies

(Supplementary Information Section 8). The materials possess yield stresses less than 10 Pa and become visibly weaker with decreasing concentration (Fig. 1e,f), although their mechanical sensitivity prevents this variation from being reliably measured. The weakness and transparency of the gels may be attributed to the narrow diameters, low concentration and limited connectivity of the fibre network.

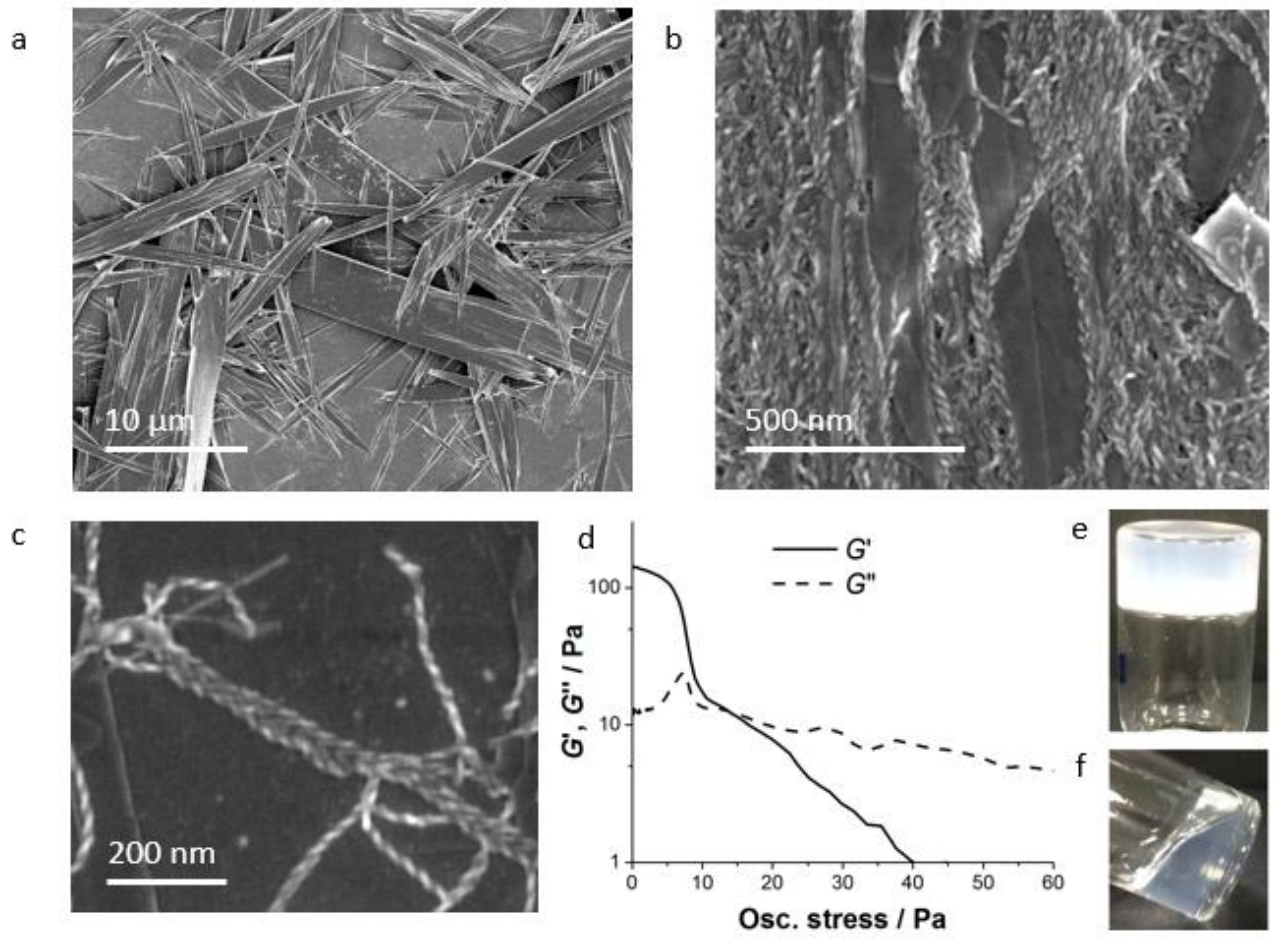


**Figure 1. SEM micrographs and rheological properties of oligo(urea) aggregates from DMF**. a,b, morphologies of the sheet-like structures formed by compounds **1** (a) and of the gel formed by compound **2**, which comprises twisted fibrils and wider ribbons (b). c, the fibrils formed by **2** entangle to form helical bundles and a variety of flat braids. d-f, mechanical properties of the gel of **2** (d). The response of a 0.3% (w/v) gel to varying shear is characteristic of a weak viscoelastic material. A 0.4% (w/v) gel passes the inversion test (e) but a 0.2% (w/v) gel is substantially weaker (f).

Helical fibrils of **2** display moderately uniform morphologies. In dried 0.3% (w/v) gels, vertical displacement profiles from atomic force microscopy (AFM) reveal a minimum fibril thickness of 2.0-2.5 nm and helical pitch of 35-40 nm (Fig. 3a,b). These findings are supported by transmission electron microscopy (TEM) images of

comparable samples, which suggest fibrils consist of single helicoids, or twisted ribbons, with diameters of 16-18 nm (Fig. 2c). Pixel intensities along 12 fibril axes were fitted to sine functions with an average pitch of 41 nm and a large standard deviation of 6 nm, indicating that the oligo(urea) assemblies are easily deformed (Supplementary Information Section 5). This flexibility or structural disorder is common among helical aggregates and likely aids the formation of entanglements, which require helical grooves that can widen to accommodate partner fibrils[17].

Powder X-ray diffraction (PXRD) studies suggest that aggregates of **1** and **2** display similar lamellar structures, with *d*-spacings of 26.2 ± 0.2 and 46.5 ± 0.5 Å, respectively (Supplementary Information Section 7). For both materials, the *d*-spacing is comparable to the length of one extended oligo(urea) molecule. Reflections at 2θ = 18.8-19.7° correspond to a *d*-spacing of 4.5-4.7 Å, matching the urea-urea distance in a typical α-tape[34]. The results are consistent with the plate-like microstructure of **1**. However, SEM images suggest that gels of **2** mostly consist of helical fibrils. These fibrils cannot be responsible for the measured reflections, as the calculated layer spacing is more than double the ribbon thickness measured in AFM experiments. Thus, the reflections are likely attributable to the minor component of flat ribbons visible in SEM images. Although these aggregates are not clearly detectable by AFM and TEM, this discrepancy likely results from the poor contrast of AFM, the inability of TEM to resolve thick nanostructures, and the need in both techniques to focus on highly dispersed sample regions.

To better understand the self-assembly pathways of **2**, atomistic molecular dynamics (MD) simulations of model assemblies were performed in Gromacs[58] using the General Amber Force Field[59] (Supplementary Information Section 11). Similar simulations have been used to probe the structures of nanotubes, bilayers and protein aggregates[60-63], and were recently exploited by our group to rationalise the scrolling behaviour of bis(urea) assemblies[64]. We noted that twisted ribbons are 4-5 times wider than the length of a gelator molecule, and likely exhibit symmetrical faces given the similarity of consecutive helix grooves. The simplest model satisfying these conditions is a layer comprising six one-dimensional arrays of hydrogen-bonded molecules, with a helical pitch of 40 nm (Fig. 2d) and no intramolecular hydrogen bonds[65]. Fibrils comprising up to four such layers were simulated for 2.5 ns, as the hydrogen bond population and helicoid morphology converged within this time.

Helical structures often display highly uniform morphologies, representing an optimal compromise between surface energy and elastic strain[16]. Simulations of the oligo(urea) helices in a vacuum at 293 K reveal that layering has little effect on hydrogen bonding: there are approximately 1.3 hydrogen bonds per carbonyl and 0.15 per pyridyl group in all simulations. However, two- and three-layer fibrils deviate greatly from the observed morphology, while a four-layer structure retains its shape and reproduces the measured ribbon thickness (Fig. 2e,f). The rows of hydrogen-bonded oligo(urea)s in our model resemble the β-sheets found in peptide fibrils[51,52], and the four-layer structure matches that of morphologically similar amyloid fibrils[66]. We hope that insights gained in this study could therefore aid our understanding of protein aggregation, which plays a central role in many important biological processes.

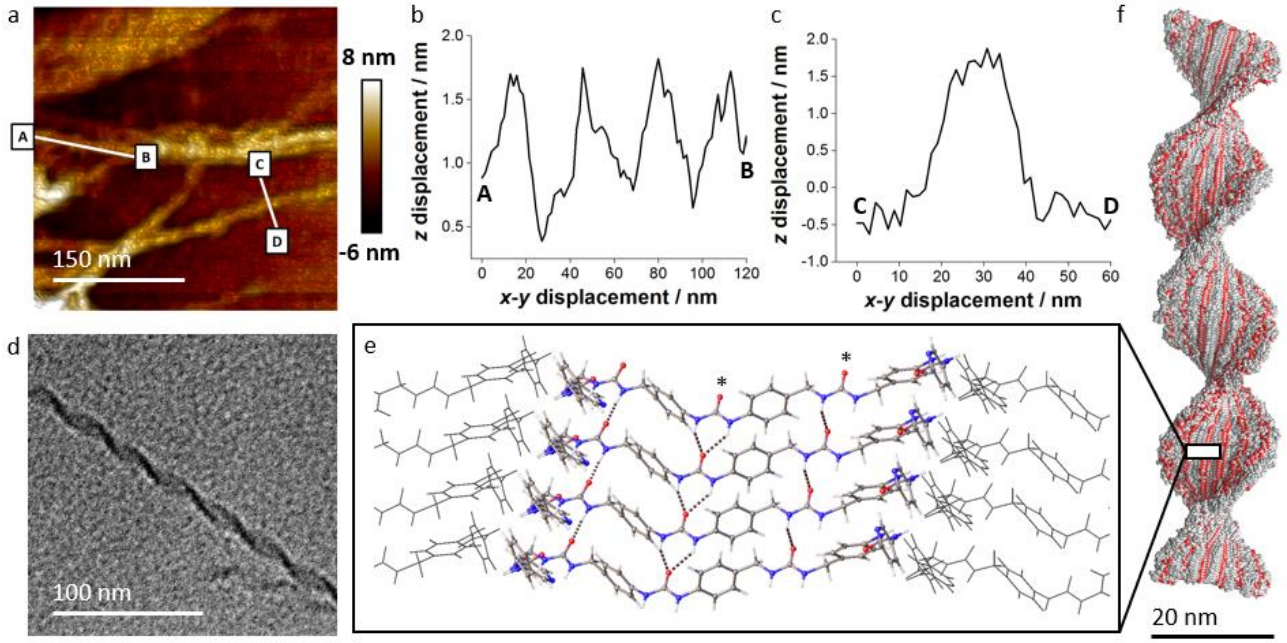


**Figure 2. Observed and simulated geometry of twisted ribbons in gels of 2.** a-c, AFM images shown in (a) suggest that the fibrils have a moderately uniform pitch, as indicated by the height map along the helical fibre between points labelled A and B (b). Thethickness of a fibril is equivalent to half a gelator molecule, as indicated in the height map between points C and D (c). d, TEM micrographs confirm that fibrils consist of single ribbons with a helicoid geometry. e,f ball and stick representation of the structure of compound **2**, derived from molecular dynamics simulations, showing that the proposed fibril structure consists of layers of oligo(urea) molecules, which lie parallel to the lamellar plane and form six parallel 1D hydrogen-bonded tapes (e). Oxygen is shown in red, nitrogen in blue, carbon in grey, and hydrogen in pale grey. The final frame of a 2.5 ns

simulation is shown as an orthographic projection (f), with the two carbonyl oxygen atoms marked with asterisks (e) displayed in red for clarity. The simulations indicate that four layers are required to produce a stable helicoid with the observed pitch and ribbon thickness.

*Helix braiding*

The periodic crossing patterns displayed by braided fibrils of **2** resemble two-dimensional colloidal crystals[67]. However, every crossing in a braid may be promoted or disfavoured by crossings already formed, making the process of braid formation analogous to an intramolecular chemical reaction. Furthermore, defects should be common given that new crossings prevent the removal or alteration of earlier entanglements. The ability of helices to form well-defined braids despite these constraints suggests that crossing patterns are tightly controlled by interhelical interactions[68]. The defect frequency determines the gel mesh size, as fibrils incorrectly integrated into developing braids produce branch points in the resulting fibre network[69]. Since braid crossings, like mechanical bonds, are topologically fixed, the resulting branch points behave as permanent junctions and the variability in branching density may be gauged from SEM images of dried gels (Fig. 3).

To better understand the braiding process, it is necessary to catalogue the observed braid topologies, defined by crossing patterns of fibrils. While mathematical techniques from knot theory have been applied to molecular knots and links[19,70], these analyses have not been extended to the few braids identified in crystallographic studies[21-25]. In braid theory, a braid is represented by parallel strands that cross under or over their neighbours[48]. A letter indicates which strands are crossed, with the case denoting whether the handedness of the crossing. For example, a crossing between the first and second strands is labelled *a* if the right strand passes over the left and *A* otherwise. The braid word is a series of letters listing the crossings in the repeat unit. Right-handed triple helices have the braid word $(ab)^3$, and $(aB)^3$ describes a three-stranded Brunnian braid, which resembles a Borromean link in that it converts to separate, non-entangled strands if any strand is removed[23,24]. It should be noted that most braids have several braid words, as certain groups of crossings can be rearranged without breaking or removing strands.

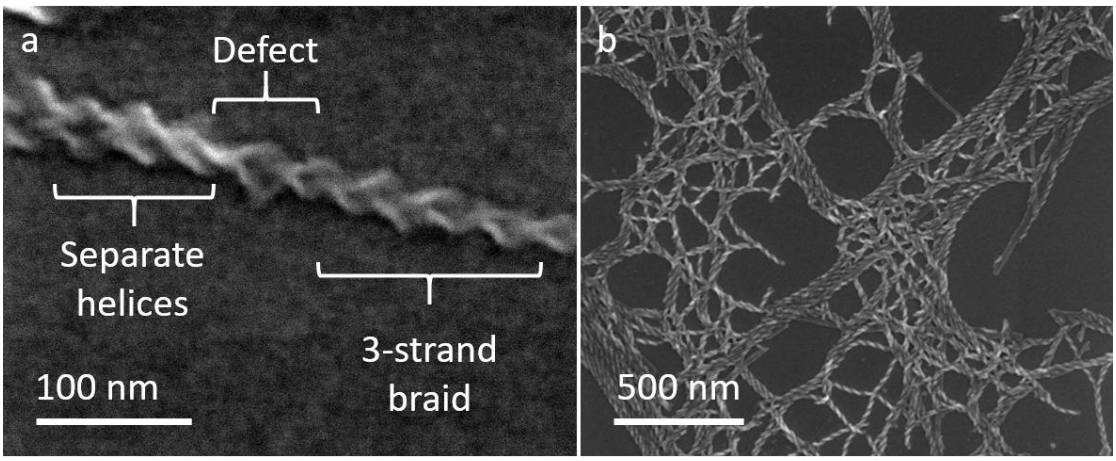


**Figure 3. SEM images illustrating branching of gel fibres due to braiding defects**. a, SEM image of a single 3-stranded braid showing a defect in which the braid separates into separate fibrils. This defect results in a branch point, increasing the branching density in the gel. b, SEM image showing that the separation of branch points in dried gel samples is highly variable.

Most braids in gels of **2** are simple and symmetrical. Helical bundles are the most common structures and invariably share the handedness of the constituent fibrils, as expected for assemblies of near-parallel helices[71]. However, flat braids of three or more strands also arise and often incorporate heterochiral fibrils. Based on these observations, we hypothesise that braiding is controlled by three rigid topological constraints. Firstly, the simplest braid word must contain an equal number of crossings for each strand (Rule 1). Secondly, crossings must be uniformly spaced and equivalent for all strands, to avoid variations in helical pitch (Rule 2). Finally, two right-handed fibrils winding around each other must form only right-handed crossings, and pairs of left-handed must do the opposite (Rule 3). A consequence of Rule 3 is that pairs of heterochiral fibrils must form crossings of alternating handedness, such that one fibril always lies above the other (Fig. 4a).

Topological constraints limit the possible braiding outcomes. Double helices are the only feasible two-stranded structures, and three fibrils must form triple helices or Brunnian braids. For four strands, an exhaustive survey reveals 354 braid words with uniformly spaced crossings, but only four structures can incorporate topologically equivalent helices (Supplementary Information Section 10). These are the quadruple helix, two nested arrays of homochiral double helices, and a similar arrangement of heterochiral double helices. The corresponding braid words are $(abc)^4$, $(abC)^4$, (*aBcaBcabCAbc*) and (*abCAbcABcaBC*), respectively. It should be

noted that homochiral and heterochiral fibrils pack differently at crossings[72]. Thus, fibrils that are topologically equivalent, displaying the same crossing sequences, are not always geometrically equivalent, and braids sharing a braid word may differ in stability.

Samples of 20 separate oligo(urea) gels, with gelator concentrations between 0.2 and 0.5% (w/v), were imaged by SEM over three regions several hundred micrometres apart. The images reveal a small number of distinct braid topologies (Fig. 4b-e), with no clear variation between gels of differing concentration. Visual assignment of braid topologies is generally difficult, but simple braids can be categorised by counting the fibrils and matching crossings to candidate structures. While entanglements between homochiral fibrils usually produce double helices and larger helical bundles, flat braids are also common. Three-stranded Brunnian braids account for the majority of flat braids and are observed to form from both homochiral and mixed-chirality fibrils. In addition, examples of nested homochiral double helices, though similar in appearance to three-stranded braids, have been tentatively identified.

The categorised braids were all highlighted as feasible structures by our braid theory analysis. For every structure observed, the braid word comprises *N* repetitions of (*N*-1) crossings. Simple braids may be favoured because new crossings are pre-organised by crossings immediately surrounding them, which encode too little information to template a complex braiding pattern. Interestingly, braids of this type cannot be Brunnian if they contain an even number of fibrils. Thus, for a large Brunnian braid to arise, an odd-stranded braid must merge with an even-stranded braid comprising homochiral fibrils. This constraint limits the potential for large flat braids and makes defect formation more probable.

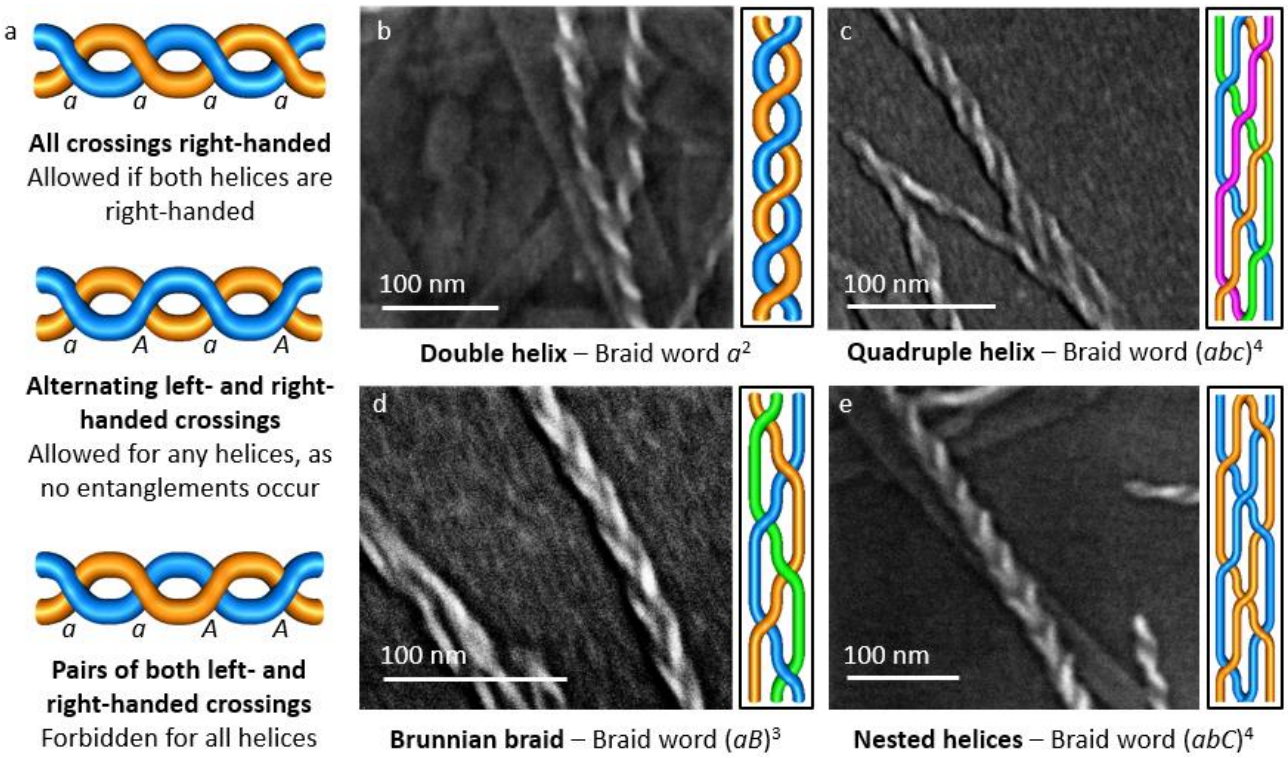


**Figure 4 SEM micrographs of braid topologies observed in gels of 2**. a, cartoon diagrams showing two-stranded entanglements and their corresponding braid words. The braid word describes which the pattern of crossings in the repeat unit, which must conform to certain topological constraints. b,c, commonly observed entanglements in gels of **2**, double helices (b) and larger helical bundles (c). d,e, three and four-stranded entanglements observed in gels of **2**, three-strand Brunnian braids (d) and tentative examples of nested homochiral double helices (e).

*Chiral amplification*

Interactions between helical fibrils strongly depend on their supramolecular chirality[73,74]. SEM images show that helical bundles cannot contain both left- and right-handed fibrils of **2**, as heterochiral helices diverge from each other after crossings arise (Fig. 5a). Remarkably, however, inversions of chirality can occur, allowing fibrils to become entangled regardless of their original handedness (Fig. 5b). Similar inversions in flat braids have not been resolved but may be necessary to optimise intercalation of helix ridges and grooves. It is clear that molecules of **2** can switch between two enantiomorphic arrangements[7,75], with an activation barrier surmountable by small changes in the fibril environment.

The handedness of the helices is also responsive to chiral additives. As an achiral LMWG, compound **2** typically forms gels containing an equal mixture of left- and right-handed fibrils. However, SEM images of four samples (Fig. 5c) indicate

that exclusively right-handed fibrils form if the hot precursor sol is filtered through cotton wool, a chiral natural product consisting predominantly of the D-glucose polymer cellulose. Circular dichroism (CD) spectra of these gels confirm the presence of net chirality, displaying a weak signal at 315 nm (Fig. 5d). The spectra provide strong evidence that the filtering treatment biases the formation of right-handed fibrils, as the signal does not appear in the spectra of two untreated gels or a treated sample of pure DMF (Supplementary Information Section 9). Linear dichroism (LD) effects[76] can be discounted given the absence of signals in control samples and the corroborating evidence of SEM images.

Several processes can induce symmetry breaking in achiral materials. Homochiral aggregates may develop from small populations of primary nuclei or through secondary nucleation by chiral impurities[77]. Alternatively, direct interactions with chiral materials may cause nascent aggregates to favour one enantiomorph[78]. These possibilities are inconsistent with the behaviour of gelator **2**. Non-stochastic primary nucleation is unlikely given that only gels produced from filtered sols show chiral amplification and gels with only left-handed fibrils are never observed. No chiral reagents are used when synthesising **2** and direct nucleation by the cotton wool filter must be minor since the gelation rate is little affected. Moreover, the absence of cotton fibres in SEM images of the gels suggests they are too sparsely distributed to significantly interact with growing fibrils.

A final possibility is that fibrils self-assemble in a cooperative fashion. A small bias of right-handed helices introduced by filtering could be amplified if these fibrils act as secondary nuclei[79,80] or invert neighbouring left-handed assemblies. Given that contact between non-entangled heterochiral helices does not affect their handedness, this process probably requires the entanglement of fibrils, as observed in SEM images (Fig. 5b). Each helix can entangle multiple fibrils to produce a cascade of inversion events, such that even a trace initial chiral bias can completely eliminate the minor enantiomorph[81,82]. This Majority Rules effect resembles the propagation of prion proteins, which are thought to replicate exponentially *via* separation of fibril bundles[83,84]. A similar mechanism could also account for the emergence of net chirality in early biological systems[85]. While speculative, the proposed mechanism of chiral amplification is consistent with the existence of multi-stranded braids. If braid crossings form through random collisions between fibrils, entanglements between three or more fibrils at a single point should be highly unlikely. Thus, it is suggested that fibrils bind together at an early stage of growth,

possibly as part of the nucleation process (Supplementary Information Section 9). A major aim of our ongoing research is to test this hypothesis by exploring the effect of seeding and other initial conditions on the aggregation outcome.

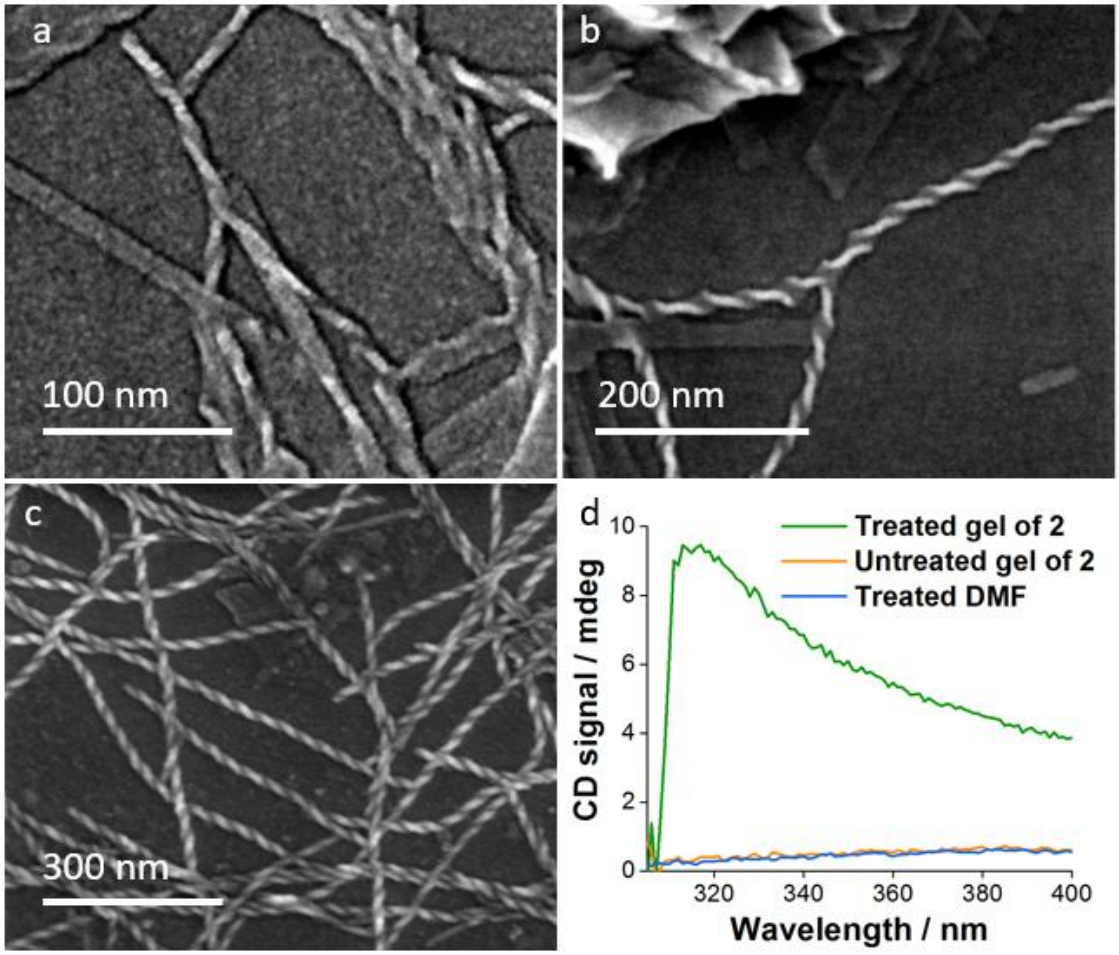


**Figure 5 Chiral amplification of oligo(urea) fibrils**. a-c, SEM images showing the dependence of entanglement on fibril chirality. Pairs of heterochiral helices cannot become entangled (a) unless one fibril undergoes a change in handedness as occurs in (b). c, SEM image showing the exclusive formation of right-handed helices through the helix inversion mechanism which promoted by trace chiral impurities in sols of **2**. d, Circular dichroism spectra of the gels, which show a net CD signal when exposed to cotton wool before gelation but no significant signal when untreated with cotton wool. In the absence of gelator the DMF solvent does not show a CD signal even when filtered through cotton wool.

Rheological fine-tuning of biomaterials involves the regulation of helix-helix interactions, and it is possible for synthetic materials to be similarly engineered[86,87]. For example, shear moduli for gels of semi-flexible helical polymers rise non-linearly with fibre thickness and persistence length[11,13]. Since they cannot form cylindrical

bundles, mixed-chirality fibrils tend to form flatter braids, which are also likely to be shorter, narrower and less abundant. Thus, the resulting gels are predicted to be less stiff than gels containing only homochiral braids. Rheological properties do not markedly differ between homochiral and mixed-chirality gels of **2**, but this could be attributed to their low yield strengths and variable concentrations of larger, untwisted ribbons. Future work will focus on developing more soluble oligo(urea)s to produce stronger and more uniform gels, in which the effects of braiding and gelator loading can be quantitatively tested.

*Conclusion*

Helical fibrils in gels of pentakis(urea) **2** form high-fidelity braids with repeated crossing patterns due to the topological constraints governing interhelical interactions. Braid theory has been used to rationalise the dominant patterns of fibre entanglements and highlight rules applicable to other networks of helical fibrils. It has been demonstrated that braids of mixed-chirality helices form more varied arrangements of crossings but may also undergo inversions of chirality to generate simple helical bundles. Building on this observation, we have shown that the oligo(urea) assemblies are highly sensitive to chiral amplification, giving rise to helices of a single handedness if the precursor sols are filtered through a chiral material. We hope that these insights will aid our understanding of biological helical fibrils and the development of supramolecular gels with biomimetic properties.

## Methods

Details of the synthesis of **1** and **2** and associated characterisation data along with spectroscopic, microscopic and computational methods are given in the Supplementary Information.

## Data Availability

All the underlying research data is available from doi: 10.15128/r2cz30ps655 in accordance with the UK research councils' open data policy, and from the corresponding authors on reasonable request.

## Acknowledgements

We thank the Engineering and Physical Sciences Research Council for funding this work *via* a Doctoral Training Studentship awarded to CDJ. We would also like to thank the Leverhulme Trust for supporting KEH *via* the Scientific Properties of Complex Knots (SPOCK) Research Programme Grant. We are grateful to Leon Bowen, Budhika Mendis and Stephen Boothroyd for their assistance in obtaining electron microscopy images and rheological data.

## Author contribution

CDJ, HTDS and KL performed the synthesis of new compounds. RLT and HTDS carried out the AFM measurements. KEH and CDJ analysed the braid topologies. CDJ completed the remaining experimental studies. JWS was responsible for overall project concept, direction and coordination. CDJ and JWS wrote the manuscript.

## Competing interests

The authors declare no competing interests.

## References

1 de Loos, M., Feringa, B. L. & van Esch, J. H. Design and application of self-assembled low molecular weight hydrogels. *Eur. J. Org. Chem.*, 3615-3631 (2005).
2 Terech, P. & Weiss, R. G. Low molecular mass gelators of organic liquids and the properties of their gels. *Chem. Rev.* **97**, 3133-3159 (1997).
3 Yashima, E. *et al.* Supramolecular Helical Systems: Helical Assemblies of Small Molecules, Foldamers, and Polymers with Chiral Amplification and Their Functions. *Chem. Rev.* **116**, 13752-13990 (2016).
4 Yang, S. *et al.* On the Origin of Helical Mesostructures. *J. Am. Chem. Soc.* **128**, 10460-10466 (2006).
5 Aggeli, A. *et al.* Hierarchical self-assembly of chiral rod-like molecules as a model for peptide beta-sheet tapes, ribbons, fibrils, and fibers. *Proc. Natl. Acad. Sci. U.S.A.* **98**, 11857-11862 (2001).
6 Kurouski, D. *et al.* Is Supramolecular Filament Chirality the Underlying Cause of Major Morphology Differences in Amyloid Fibrils? *J. Am. Chem. Soc.* **136**, 2302-2312 (2014).
7 Usov, I., Adamcik, J. & Mezzenga, R. Polymorphism Complexity and Handedness Inversion in Serum Albumin Amyloid Fibrils. *ACS Nano* **7**, 10465-10474 (2013).
8 Xing, K. *et al.* Triple Helical Molecular Braid and Parallel Packed Wavy Chain-Based Supramolecular Organic Frameworks with Conformation- and Packing-Dependent Luminescent Properties. *Cryst. Growth Des.* **16**, 4727-4735 (2016).
9 Weiss, J., Jahnke, E., Severin, N., Rabe, J. P. & Frauenrath, H. Consecutive conformational transitions and deaggregation of multiple-helical poly(diacetylene)s. *Nano Lett.* **8**, 1660-1666 (2008).

10 Piechocka, I. K. *et al.* Multi-scale strain-stiffening of semiflexible bundle networks. *Soft Matter* **12**, 2145-2156 (2016).
11 Jaspers, M. *et al.* Ultra-responsive soft matter from strain-stiffening hydrogels. *Nature Commun.* **5**, 5808 (2014).
12 Pritchard, R. H., Huang, Y. Y. & Terentjev, E. M. Mechanics of biological networks: from the cell cytoskeleton to connective tissue. *Soft Matter* **10**, 1864-1884 (2014).
13 Gardel, M. L. *et al.* Elastic Behavior of cross-linked and bundled actin networks. *Science* **304**, 1301-1305 (2004).
14 Burchard, W. Networks in nature. *Brit. Polym. J.* **17**, 154-163 (1985).
15 Everaers, R. *et al.* Rheology and microscopic topology of entangled polymeric liquids. *Science* **303**, 823-826 (2004).
16 Armon, S., Aharoni, H., Moshe, M. & Sharon, E. Shape selection in chiral ribbons: from seed pods to supramolecular assemblies. *Soft Matter* **10**, 2733-2740 (2014).
17 De Abreu, F. V., Dias, R. G. & von Ferber, C. Pseudo-knots in helical structures. *Soft Matter* **4**, 731-734 (2008).
18 Serna, P., Bunin, G. & Nahum, A. Topological Constraints in Directed Polymer Melts. *Phys. Rev. Lett.* **115**, 5 (2015).
19 Horner, K. E., Miller, M. A., Steed, J. W. & Sutcliffe, P. M. Knot theory in modern chemistry. *Chem. Soc. Rev.* **45**, 6432-6448 (2016).
20 Fielden, S. D. P., Leigh, D. A. & Woltering, S. L. Molecular Knots. *Angew. Chem. Int. Ed.* **56**, 11166-11194 (2017).
21 Alvariño, C., Simond, D., Lorente, P. M., Besnard, C. & Williams, A. F. Chains, Necklaces and Weaving Chain-link Grids from Self-Assembly Reactions. *Chem. Eur. J.* **21**, 8851-8858 (2015).
22 Yang, G. P., Hou, L., Luan, X. J., Wu, B. A. & Wang, Y. Y. Molecular braids in metal-organic frameworks. *Chem. Soc. Rev.* **41**, 6992-7000 (2012).
23 Zhang, J. P., Qi, X. L., He, C. T., Wang, Y. & Chen, X. M. Interweaving isomerism and isomerization of molecular chains. *Chem. Commun.* **47**, 4156-4158 (2011).
24 Byrne, P., Lloyd, G. O., Clarke, N. & Steed, J. W. A "Compartmental" borromean weave coordination polymer exhibiting saturated hydrogen bonding to anions and water cluster inclusion. *Angew. Chem. Int. Ed.* **47**, 5761-5764 (2008).
25 Luan, X. J. *et al.* An investigation of the self-assembly of neutral, interlaced, triple-stranded molecular braids. *Chem. Eur. J.* **12**, 6281-6289 (2006).
26 Ashley, C. W. *The Ashley Book of Knots*. 471-510 (Doubleday, 1944).
27 Danon, J. J. *et al.* Braiding a molecular knot with eight crossings. *Science* **355**, 159-162 (2017).
28 Sułkowska, J. I. *et al.* Knotting pathways in proteins. *Biochem. Soc. Trans.* **41**, 523-527 (2013).
29 Taylor, W. R. Protein knots and fold complexity: Some new twists. *Comput. Biol. Chem.* **31**, 151-162 (2007).
30 Damasceno, P. F., Engel, M. & Glotzer, S. C. Predictive Self-Assembly of Polyhedra into Complex Structures. *Science* **337**, 453-457 (2012).
31 Manoharan, V. N., Elsesser, M. T. & Pine, D. J. Dense packing and symmetry in small clusters of microspheres. *Science* **301**, 483-487 (2003).
32 Whitesides, G. M. & Grzybowski, B. Self-assembly at all scales. *Science* **295**, 2418-2421 (2002).
33 Meng, S. C., Tang, Y. Q., Yin, Y., Yin, X. L. & Xie, J. M. A theoretical study of molecular conformations and gelation ability of N,N '-dipyridyl urea compounds in ethanol solution: DFT calculations and MD simulations. *RSC Adv.* **3**, 18115-18127 (2013).

34 van Esch, J., DeFeyter, S., Kellogg, R. M., DeSchryver, F. & Feringa, B. L. Self-assembly of bisurea compounds in organic solvents and on solid substrates. *Chem. Eur. J.* **3**, 1238-1243 (1997).
35 Jones, J. E. *et al.* Length-Dependent Formation of Transmembrane Pores by 310-Helical α-Aminoisobutyric Acid Foldamers. *J. Am. Chem. Soc.* **138**, 688-695 (2016).
36 Piguet, C., Bernardinelli, G. & Hopfgartner, G. Helicates as Versatile Supramolecular Complexes. *Chem. Rev.* **97**, 2005-2062 (1997).
37 King, P. J. S. *et al.* A modular self-assembly approach to functionalised [small beta]-sheet peptide hydrogel biomaterials. *Soft Matter* **12**, 1915-1923 (2016).
38 Saiani, A. *et al.* Self-assembly and gelation properties of alpha-helix versus beta-sheet forming peptides. *Soft Matter* **5**, 193-202 (2009).
39 Nagarkar, R. P., Hule, R. A., Pochan, D. J. & Schneider, J. P. De novo design of strand-swapped beta-hairpin hydrogels. *J. Am. Chem. Soc.* **130**, 4466-4474 (2008).
40 Escuder, B., Rodríguez-Llansola, F. & Miravet, J. F. Supramolecular gels as active media for organic reactions and catalysis. *New J. Chem.* **34**, 1044-1054 (2010).
41 Steed, J. W. Anion-tuned supramolecular gels: a natural evolution from urea supramolecular chemistry. *Chem. Soc. Rev.* **39**, 3686-3699 (2010).
42 Foster, J. A. *et al.* Pharmaceutical polymorph control in a drug-mimetic supramolecular gel. *Chem. Sci.* **8**, 78-84 (2017).
43 Foster, J. A. *et al.* Anion-switchable supramolecular gels for controlling pharmaceutical crystal growth. *Nature Chem.* **2**, 1037-1043 (2010).
44 Catrouillet, S. *et al.* Patchy Supramolecular Bottle-Brushes Formed by Solution Self-Assembly of Bis(urea)s and Tris(urea)s Decorated by Two Incompatible Polymer Arms. *Langmuir* **32**, 8900-8908 (2016).
45 Aisenbrey, C., Pendem, N., Guichard, G. & Bechinger, B. Solid state NMR studies of oligourea foldamers: Interaction of N-15-labelled amphiphilic helices with oriented lipid membranes. *Org. Biomol. Chem.* **10**, 1440-1447 (2012).
46 Stanley, C. E. *et al.* Anion binding inhibition of the formation of a helical organogel. *Chem. Commun.*, 3199-3201 (2006).
47 de Loos, M. *et al.* Tripodal Tris-Urea Derivatives as Gelators for Organic Solvents. *Eur. J. Org. Chem.* **2000**, 3675-3678 (2000).
48 Artin, E. Theory of braids. *Annals of Mathematics* **48**, 101-125 (1947).
49 Coubrough, H. M., Jones, C. D., Yufit, D. S. & Steed, J. W. Gelation by histidine-derived ureas. *Supramol. Chem.* **30**, 384-394 (2018).
50 James, S. J., Perrin, A., Jones, C. D., Yufit, D. S. & Steed, J. W. Highly interlocked anion-bridged supramolecular networks from interrupted imidazole-urea gels. *Chem. Commun.* **50**, 12851-12854 (2014).
51 Dzwolak, W. Chirality and Chiroptical Properties of Amyloid Fibrils. *Chirality* **26**, 580-587 (2014).
52 Serpell, L. C. Alzheimer's amyloid fibrils: structure and assembly. *Biochim. Biophys. Acta* **1502**, 16-30 (2000).
53 Duspara, P. A., Islam, M. S., Lough, A. J. & Batey, R. A. Synthesis and Reactivity of N-Alkyl Carbamoylimidazoles: Development of N-Methyl Carbamoylimidazole as a Methyl Isocyanate Equivalent. *J. Org. Chem.* **77**, 10362-10368 (2012).
54 Meazza, L. *et al.* Halogen-bonding-triggered supramolecular gel formation. *Nature Chem.* **5**, 42-47 (2013).
55 Piepenbrock, M. O. M., Clarke, N. & Steed, J. W. Shear induced gelation in a copper(II) metallogel: new aspects of ion-tunable rheology and gel-reformation by external chemical stimuli. *Soft Matter* **6**, 3541-3547 (2010).
56 Todd, A. M., Anderson, K. M., Byrne, P., Goeta, A. E. & Steed, J. W. Helical or Polar Guest-Dependent Z' = 1.5 or Z' = 2 Forms of a Sterically Hindered Bis(urea) Clathrate. *Cryst. Growth Des.* **6**, 1750-1752 (2006).

57 Terech, P., Pasquier, D., Bordas, V. & Rossat, C. Rheological Properties and Structural Correlations in Molecular Organogels. *Langmuir* **16**, 4485-4494 (2000).
58 Van der Spoel, D. *et al.* GROMACS: Fast, flexible, and free. *J. Comput. Chem.* **26**, 1701-1718 (2005).
59 Case, D. A. *et al.* The Amber Biomolecular Simulation Programs. *J. Comput. Chem.* **26**, 1668-1688 (2005).
60 Pyrlin, S. V., Hine, N. D. M., Kleij, A. W. & Ramos, M. M. D. Self-assembly of bis-salphen compounds: from semiflexible chains to webs of nanorings. *Soft Matter* **14**, 1181-1194 (2018).
61 Eckes, K. M., Mu, X., Ruehle, M. A., Ren, P. & Suggs, L. J. β Sheets Not Required: Combined Experimental and Computational Studies of Self-Assembly and Gelation of the Ester-Containing Analogue of an Fmoc-Dipeptide Hydrogelator. *Langmuir* **30**, 5287-5296 (2014).
62 Forman, C. J., Fejer, S. N., Chakrabarti, D., Barker, P. D. & Wales, D. J. Local Frustration Determines Molecular and Macroscopic Helix Structures. *J. Phys. Chem. B* **117**, 7918-7928 (2013).
63 Huang, M.-J., Kapral, R., Mikhailov, A. S. & Chen, H.-Y. Coarse-grain model for lipid bilayer self-assembly and dynamics: Multiparticle collision description of the solvent. *J. Chem. Phys.* **137**, 055101 (2012).
64 Jones, C. D., Kennedy, S. R., Walker, M., Yufit, D. S. & Steed, J. W. Scrolling of Supramolecular Lamellae in the Hierarchical Self-Assembly of Fibrous Gels. *Chem* **3**, 603-628 (2017).
65 Núñez-Villanueva, D. *et al.* H-Bond Self-Assembly: Folding versus Duplex Formation. *J. Am. Chem. Soc.* **139**, 6654-6662 (2017).
66 Fitzpatrick, A. W. P. *et al.* Atomic structure and hierarchical assembly of a cross-β amyloid fibril. *Proc. Natl. Acad. Sci. U.S.A.* **110**, 5468 (2013).
67 Velikov, K. P., Christova, C. G., Dullens, R. P. A. & van Blaaderen, A. Layer-by-layer growth of binary colloidal crystals. *Science* **296**, 106-109 (2002).
68 Baumgartner, R., Fu, H., Song, Z., Lin, Y. & Cheng, J. Cooperative polymerization of α-helices induced by macromolecular architecture. *Nature Chem.* **9**, 614-622 (2017).
69 Müller, M. F., Ris, H. & Ferry, J. D. Electron microscopy of fine fibrin clots and fine and coarse fibrin films. *J. Mol. Biol.* **174**, 369-384 (1984).
70 Fielden Stephen, D. P., Leigh David, A. & Woltering Steffen, L. Molecular Knots. *Angew. Chem. Int. Ed.* **56**, 11166-11194 (2017).
71 Xu, F. *et al.* Self-Assembly of Left- and Right-Handed Molecular Screws. *J. Am. Chem. Soc.* **135**, 18762-18765 (2013).
72 Sia, S. K. & Kim, P. S. A Designed Protein with Packing between Left-Handed and Right-Handed Helices. *Biochemistry* **40**, 8981-8989 (2001).
73 Morrow, S. M., Bissette, A. J. & Fletcher, S. P. Transmission of chirality through space and across length scales. *Nature Nanotechnol.* **12**, 410-419 (2017).
74 Duan, P., Cao, H., Zhang, L. & Liu, M. Gelation induced supramolecular chirality: chirality transfer, amplification and application. *Soft Matter* **10**, 5428-5448 (2014).
75 Tomsett, M. *et al.* A tendril perversion in a helical oligomer: trapping and characterizing a mobile screw-sense reversal. *Chem. Sci.* **8**, 3007-3018 (2017).
76 Dafforn, T. R. & Rodger, A. Linear dichroism of biomolecules: which way is up? *Curr. Opin. Struct. Biol.* **14**, 541-546 (2004).
77 Ribó, J. M., Hochberg, D., Crusats, J., El-Hachemi, Z. & Moyano, A. Spontaneous mirror symmetry breaking and origin of biological homochirality. *J. R. Soc. Interface* **14**, 20170699 (2017).

78 Palmans Anja, R. A., Vekemans Jef, A. J. M., Havinga Edsko, E. & Meijer, E. W. Sergeants-and-Soldiers Principle in Chiral Columnar Stacks of Disc-Shaped Molecules with C3 Symmetry. *Angew. Chem. Int. Ed.* **36**, 2648-2651 (2003).
79 Ogi, S., Sugiyasu, K., Manna, S., Samitsu, S. & Takeuchi, M. Living supramolecular polymerization realized through a biomimetic approach. *Nature Chem.* **6**, 188-195 (2014).
80 Azeroual, S. *et al.* Mirror symmetry breaking and chiral amplification in foldamer-based supramolecular helical aggregates. *Chem. Commun.* **48**, 2292-2294 (2012).
81 Prins, L. J., Timmerman, P. & Reinhoudt, D. N. Amplification of chirality: The "sergeants and soldiers" principle applied to dynamic hydrogen-bonded assemblies. *J. Am. Chem. Soc.* **123**, 10153-10163 (2001).
82 Langeveld-Voss, B. M. W., Waterval, R. J. M., Janssen, R. A. J. & Meijer, E. W. Principles of "majority rules" and "sergeants and soldiers" applied to the aggregation of optically active polythiophenes: Evidence for a multichain phenomenon. *Macromolecules* **32**, 227-230 (1999).
83 Petkova, A. T. *et al.* Self-Propagating, Molecular-Level Polymorphism in Alzheimer's ß-Amyloid Fibrils. *Science* **307**, 262 (2005).
84 Masel, J., Jansen, V. A. A. & Nowak, M. A. Quantifying the kinetic parameters of prion replication. *Biophys. Chem.* **77**, 139-152 (1999).
85 Ruiz-Mirazo, K., Briones, C. & de la Escosura, A. Prebiotic Systems Chemistry: New Perspectives for the Origins of Life. *Chem. Rev.* **114**, 285-366 (2014).
86 Hule, R. A., Nagarkar, R. P., Hammouda, B., Schneider, J. P. & Pochan, D. J. Dependence of Self-Assembled Peptide Hydrogel Network Structure on Local Fibril Nanostructure. *Macromolecules* **42**, 7137-7145 (2009).
87 Ozbas, B., Kretsinger, J., Rajagopal, K., Schneider, J. P. & Pochan, D. J. Salt-Triggered Peptide Folding and Consequent Self-Assembly into Hydrogels with Tunable Modulus. *Macromolecules* **37**, 7331-7337 (2004).

## Graphical Abstract

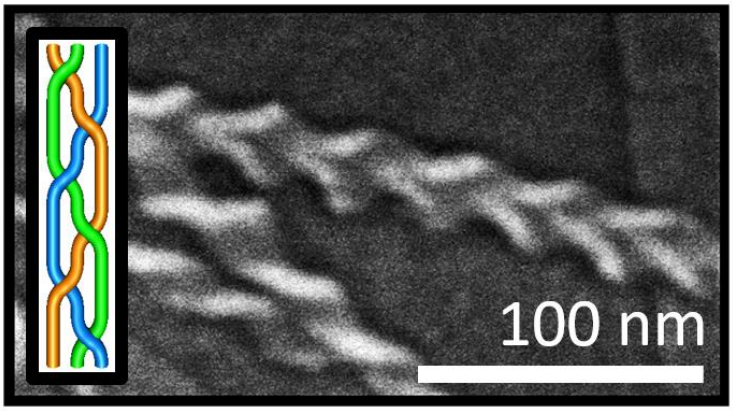


## Summary for Table of Contents

Helical structures play important roles in biological processes, yet their aggregation into fibres — which can in turn form gels — is poorly understood. Now, the self-assembly of a linear pentakis(urea) into helices that further intertwine into well-defined braided structures has been described and analysed through braid theory. Homochiral gels may be formed by exposing the precursor sol to a chiral material.